Journal of Alloys and Compounds 862 (2021) 158670

Contents lists available at ScienceDirect

Journal of Alloys and Compounds

journal homepage: www.elsevier.com/locate/jalcom

Facile synthesis of highly efficient and cost-effective photo-Fenton catalyst by ball milling commercial TiO_2 and natural magnetite

Qi Jiang[a,d], Runliang Zhu[a,b,c,*]

[a] CAS Key Laboratory of Mineralogy and Metallogeny, Guangdong Provincial Key Laboratory of Mineral Physics and Materials, Guangzhou Institute of Geochemistry, Chinese Academy of Sciences, Guangzhou 510640, China
[b] Institutions of Earth Science, Chinese Academy of Sciences, Beijing 100049, China
[c] University of Chinese Academy of Sciences, Beijing 100049, China
[d] College of Environment & Ecology, Xiamen University, Xiamen 361021, China

ARTICLE INFO

Article history:
Received 28 October 2020
Received in revised form 24 December 2020
Accepted 6 January 2021
Available online 8 January 2021

Keywords:
Photo-Fenton
Ball milling
Mag
TiO_2/Mag composites
H_2O_2

ABSTRACT

Heterogeneous Fenton reaction is a usable technique to remove organic contaminants in water, while developing highly efficient and cost-effective catalysts with simple preparation method is critical for its practical application. In this work, novel TiO_2/Mag composites were prepared from commercial TiO_2 and natural magnetite (Mag) via a facile ball milling process. We expect the obtained composites to be efficient photo-Fenton catalysts, as photo-generated electrons from TiO_2 can be transferred to Mag to accelerate the reduction of Fe(III) to Fe(II), promoting the decomposition of H_2O_2 and production of ·OH. Structural characterization results exhibited ball milling could not change mineral phases of both TiO_2 and Mag. TiO_2/Mag composites remained good magnetic saturation and could be rapidly separated from reaction medium. In degrading cefotaxime, TiO_2/Mag composites showed high photo-Fenton catalytic activities, with the degradation rate by 10%TiO_2/Mag at near neutral pH of 5.6 being about 11.6 and 8.2 times higher than that of natural and ball-milled Mag, respectively. Moreover, even at low H_2O_2 concentration of 1 mmol/L, 10%TiO_2/Mag remained relatively high photo-Fenton catalytic activity when compared to natural and ball-milled Mag. The better production of ·OH in the photo-Fenton system catalyzed by 10%TiO_2/Mag (0.244 mmol/L) than that by natural and ball-milled Mag (0.049 and 0.064 mmol/L) also illustrated efficient utilization of H_2O_2 by 10%TiO_2/Mag. Above results well support our hypothesis that photo-generated electrons from TiO_2 were transferred to Mag, which then benefited the Fenton reactivity of Mag and degradation of cefotaxime. In all, TiO_2/Mag composites prepared by ball milling have promising practical application in water treatment, thanks to their merits such as high photo-Fenton catalytic activity, facile preparation, cost-effective, easy magnetic separation, good stability, suitable for near neutral pH, and efficient utilization of H_2O_2.

1. Introduction

As one of the most studied advanced oxidation processes (AOPs), Fenton reaction has many advantages for combating toxic and recalcitrant organic contaminants, such as mild operating condition, easy operation, and environmental friendliness [1–3]. However, slow recovery rate of Fe(II) from Fe(III) inevitably weakens the performance of Fenton reaction in water treatment, which also consumes a large amount of H_2O_2 and inhibits the production of ·OH [4,5]. Several studies attempted to increase the efficiency of Fenton reaction in degrading contaminants. For example, the addition of light irradiation (< 580 nm) in Fenton reaction can quicken the reduction of Fe(II) through the photolysis of Fe(III) [6,7]; and electrochemical reaction can promote the conversion of Fe(II)/Fe(III) in Fenton reaction by regenerating Fe(II) on the cathode [8,9]. In particular, the combination of photocatalysis with Fenton reaction is able to continuously transfer photo-generated electrons into Fenton reaction, leading to the obvious acceleration of Fe(II)/Fe(III) cycle and enhancement of contaminants removal [10–12]. In addition to achieving high efficiency, a financially affordable Fenton reaction apparently has excellent practical application potentials for removing contaminants from water, which mainly depends on the adopted catalysts.

* Corresponding author at: CAS Key Laboratory of Mineralogy and Metallogeny, Guangdong Provincial Key Laboratory of Mineral Physics and Materials, Guangzhou Institute of Geochemistry, Chinese Academy of Sciences, Guangzhou 510640, China.
E-mail address: zhurl@gig.ac.cn (R. Zhu).

https://doi.org/10.1016/j.jallcom.2021.158670
0925-8388/

For the purpose of reducing costs of Fenton reaction, it is essential to use low-cost raw materials to prepare catalysts via facile and available methods. Given the abundance in nature, natural magnetite (Mag) is regarded as a cheap and readily available iron mineral [13,14]. The co-existence of Fe(III) and Fe(II) in Mag facilitates the transfer of electrons to H_2O_2 by Fe(II)/Fe(III) cycle, thus bringing about a good Fenton degradation of contaminants [1,15,16]. Matta et al. found Fe(III)-containing oxides (e.g. hematite, goethite, lepidocrocite or ferrihydrite) were less effective than Mag in Fenton degradation of 2, 4, 6-trinitrotoluene [17]. Beyond Fe(III) and Fe(II), some low-proportion transition metal ions also present in natural Mag, such as Ti(IV) and V(III), which may contribute to enhancing its Fenton catalytic activity [18,19]. Moreover, because of strong ferromagnetism, natural Mag can be rapidly separated from reaction medium at low costs [4]; this readily recoverability is of great significance in water treatment. In all, based on above outstanding properties, natural Mag is an ideal Fenton catalyst with promising practical applications. Despite of such advantages, the demand for increasing the Fenton catalytic activity of natural Mag is always the ongoing priority for its practical applications. Especially the consumption of Fe(II) during Fenton process is much faster than its regeneration by H_2O_2, leading to a gradually decrease of Fenton catalytic activity. Besides, the utilization efficiency of H_2O_2 should be enhanced to further cut down the costs from H_2O_2 consumption.

In order to further improve the Fenton catalytic activity, semiconductors are recommended to combine with Fenton catalysts. The introduction of semiconductors (e.g. TiO_2, $BiVO_4$, and graphene oxide) is conducive to accelerating the conversion of Fe(II)/Fe(III) in photo-Fenton reaction through continuous transfer of photo-generated electrons to Fenton catalysts [20–22], and then promoting the decomposition of H_2O_2 and production of ·OH. This is basically the same as the synergistic effect between photocatalysis and Fenton reaction. Moreover, Zhu et al. [23,24] noted that, rely on a similar strategy, Ag/AgX/ferrihydrite (Cl, Br) showed favorable photo-Fenton catalytic activity in degrading bisphenol A even at near neutral pH, and such activity was less affected by the decreased concentration of initial H_2O_2. Therefore, we propose that combining photocatalysts (e.g.,TiO_2) with natural Mag may develop a cost-effective, highly efficient, and magnetically separable photo-Fenton catalyst for water treatment, which can also achieve the efficient utilization of H_2O_2 and near neutral pH application. In addition, directly using commercially available photocatalysts and employing the ball milling method to combine photocatalysts with Mag should be able to further reduce the costs of Fenton catalysts. Meanwhile, iron mineral and TiO_2 may be combined through the formation of Fe-O-Ti bond after the ball milling process [25], which also contributes to the transfer of photo-generated electrons between them.

In this work, with the precursors of commercial TiO_2 and natural Mag, we have synthesized TiO_2/Mag composites by a simple solvent-free ball milling approach. The structural and magnetic properties of the as-synthesized samples were characterized. As a result of synergetic effects between the TiO_2-based photocatalysis and Mag-based Fenton reaction, TiO_2/Mag composites exhibited high photo-Fenton catalytic activities in degrading cefotaxime. By carefully investigating the effects of initial pH and H_2O_2 concentration, decomposition of H_2O_2, production of ·OH, and generation of Fe (II) in solutions, we clarified the synergistic mechanisms in the UV+TiO_2/Mag+H_2O_2 system and summarized typical advantages of TiO_2/Mag composites.

2. Experimental section

2.1. Materials

TiO_2(P25) Aeroxide® (79% anatase and 21% rutile, 20–80 nm) was supplied by Evonik industries, Germany. Natural Mag (70.90% Fe, 0.89% Mo, 0.27% Ti, 0.18% Ba, 0.15% Ni, 0.15% Sr, 0.12% Zn, 0.10% Al, 0.05% Rb, and 0.04% V) was acquired from Shaanxi Province in China, and was ground and sieved 600 mesh (0.023 mm). Clearly, this natural Mag contains negligible toxic elements and can be applied as Fenton catalyst. Cefotaxime (97%) was obtained by J&K Scientific Ltd. If not stated otherwise, other reagents were purchased from Aladdin and were of analytical grade. All solutions were prepared using deionized water (Millipore Corp., 18.25 MΩ cm). Whether on solids or in solutions, ferrous and ferric irons in this study were denoted as Fe(II) and Fe(III), respectively.

2.2. Synthesis of TiO_2/Mag composites

TiO_2/Mag composites were synthesized under solvent-free conditions using a planetary ball mill (Fritsch Pulverisette 6, Germany). 10 mm diameter corundum balls were employed as the milling medium. The mass ratio of balls to the mixture of TiO_2 and Mag remained constant at 10:1. Mechanical milling was implemented at 250 rpm for 20 min in a corundum pot. The TiO_2/Mag mass ratios of the mixture were 3%, 6%, 10%, and 15%, respectively. In comparative study, pure TiO_2 and Mag was ball milled via the same procedure as well.

2.3. Characterizations of TiO_2/Mag composites

The crystal phases of samples were determined by an X-ray diffractometer (XRD, Bruker D8 ADVANCE, Germany). The Specific surface area (SSA) values of samples were characterized from N_2 adsorption-desorption isotherms by Brunauer-Emmett-Teller (BET) model using Micromeritics ASAP2020 apparatus, USA. The morphologies of samples were observed using a scanning electron microscope (SEM, Phenom XL, China) with an energy dispersive X-ray (EDX). The magnetic parameters of samples were recorded by a vibrating sample magnetometer (VSM, MPMS-XL-7 Quantum Design, USA) at room temperature.

2.4. Catalytic experiments and analytical methods

The degradation of cefotaxime by catalytic processes was conducted in a photochemical reaction instrument (PCX50A Discover, Perfect Light, China). A 5 W LED lamp with maximum wavelength at 365 nm was employed as light source. Before irradiation, a dispersion of 0.2 g/L catalyst and 50 mL of 0.4 mmol/L cefotaxime aqueous solution was vigorously stirred in the dark for 30 min to attain adsorption-desorption equilibrium. After that, H_2O_2 was added, and the lamp was turned on to begin the reaction. The reaction was operated at inherent solution pH of 5.6 and 10 mmol/L H_2O_2 unless otherwise stated. If necessary, 0.1 mol/L NaOH and HNO_3 were adopted to adjust the initial pH of reaction solutions. The experiments run at least twice in parallel, and the obtained average values were used, as well as the error bars were used to represent the corresponding standard errors. To investigate catalytic stability of TiO_2/Mag composites, a recycling study was performed with samples collected from the last test in each cycle. The tested processes were the same as catalytic experiments. After being filtered by 0.22 μm micro-filtration membrane, washed with deionized water, and dried at room temperature, the recollected samples were used in next reaction.

The aqueous concentration of cefotaxime after catalysts being filtered through 0.22 μm micro-filtration membrane was analyzed by liquid chromatography (LC, Agilent 1260, USA). An Inertsil ODS column (4.6 × 150 mm, 5 μm particle size, Shimadzu, Japan) was used for chromatographic separation at 30 °C with 65% of mobile phase A (0.05 mol/L phosphate buffer) and 35% of mobile phase B (HPLC grade methanol). The injection volume was 20 μL, the flow rate of mobile phases was 0.5 mL/min, as well as the detection

wavelength was selected at 254 nm. The degradation rate of cefotaxime was fitted using a pseudo-first order model and calculated via Eq. (1) [26].

$$C_t = C_0 exp(-kt) \quad (1)$$

Here C_0, C_t and k were the concentration of cefotaxime at reaction time 0 and t (min), and rate constant of pseudo-first-order reaction (min^{-1}), respectively. The total organic carbon (TOC) of cefotaxime was monitored using a total organic carbon analyzer (TOC-V CPH, Shimadzu, Japan).

The consumption of H_2O_2 was detected by a typical spectrophotometric technology with 10 mmol/L titanium oxalate solution containing 2.4 mol/L H_2SO_4 [22]. To determine the contribution of various oxygen reactive species in catalytic systems, potassium iodide (KI, 2 mmol/L), sodium azide (NaN_3, 2 mmol/L), and benzoquinone (BQ, 2 mmol/L) were used as scavengers for ·OH, O_2^1, and $\cdot O_2^-$, respectively [27]. The oxidation of benzoic acid to *p*-hydroxybenzoic was carried out as a probe reaction for quantifying the production of ·OH [28], and the detailed information could be found in the Supplementary Material. The density of Fe(II) in solutions was determined by a modified phenanthroline spectrophotometric method through 1 g/L ammonium fluoride eliminating the interference of Fe (III), as depicted in the environmental quality standard for surface water of China (GB 3838–2002).

3. Results and discussion

3.1. The structural and magnetic characteristics of TiO_2/Mag composites

Fig. 1 showed XRD patterns of the samples. The reflections of natural Mag well corresponded to those of standard Fe_3O_4 (JCPDS no. 19–0629), indicating high purity of natural Mag. The same results in XRD spectra of ball-milled Mag as those of natural Mag demonstrated the ball milling process almost has no apparent effect on crystal phase of Mag [29,30]. Besides, the reflections of TiO_2(P25) were indexed to anatase phase (JCPDS no. 21–1272) or rutile phase (JCPDS no. 21–1276) of TiO_2. After ball milling, no new reflections were appeared on TiO_2, but the intensity of its reflections diminished marginally. The reason might be the ball milling process decreased the crystallinity of TiO_2, while a broad and amorphous phase signal emerged [31]. In TiO_2/Mag composites, primary structure of both TiO_2 and Mag were maintained. With the increase of TiO_2 loading amount from 3% to 15%, the intensities of TiO_2 reflections on TiO_2/Mag composites became stronger.

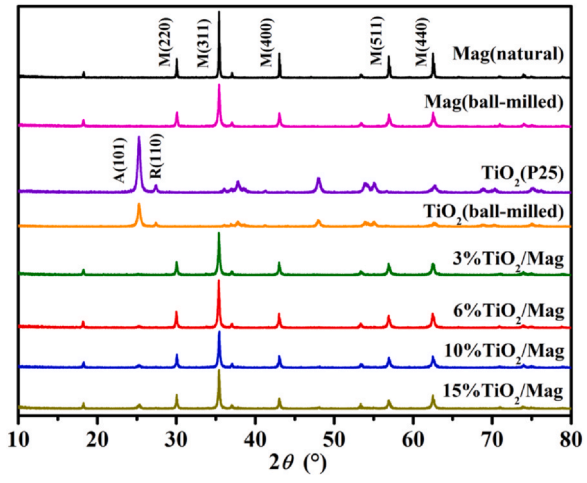

Fig. 1. XRD patterns of Mag(natural), Mag(ball-milled), TiO_2(P25), TiO_2(ball-milled), 3%TiO_2/Mag, 6%TiO_2/Mag, 10%TiO_2/Mag, and 15%TiO_2/Mag. (A=Anatase, R=Rutile, M=Magnetite.).

Using BET approach, the SSA values of Mag and TiO_2 before and after ball milling were calculated, and their values increased from 0.70 to 1.99 m^2/g and from 56.00 to 57.18 m^2/g, respectively (Table S1). Because the SSA value of TiO_2 was evidently larger than that of Mag, the SSA values of TiO_2/Mag composites enhanced from 2.92 to 5.64 m^2/g with TiO_2 amount raising from 3% to 15%.

The morphologies of samples were observed by SEM. From Fig. 2(a), natural Mag was characterized by bulky structure, irregular shape, and smooth surface, while the particles were in size of 10–50 μm approximately. A comparison between natural and ball-milled Mag exhibited a reduced particle size in the latter (less than 20 μm) (Fig. 2(a) and (b)). The morphologies of TiO_2 before and after ball milling showed few changes, and their particle sizes were about 20–80 nm (Fig. S1(a) and (c)). Due to the extremely small particle size of TiO_2 at nano-meter scope, the particle size of 10%TiO_2/Mag was near to that of ball-milled Mag (Fig. 2(b) and (c)). The results of EDS analyses (Fig. S1(b)(d) and S2) indicated the corresponding elements on natural Mag (Fe and O), ball-milled Mag (Fe and O), TiO_2(P25) (Ti and O), ball-milled TiO_2 (Ti and O), and 10%TiO_2/Mag (Ti, Fe, and O) could be detected with random selection.

As revealed by VSM measurements at room temperature (Fig. 3), the tested samples presented typical super-paramagnetic features with relatively low coercivity and remanence (the left-upper inset of Fig. 3(a)) [32,33]. Natural Mag had a magnetic saturation (MS) value at 60.6 emu/g, while it decreased to 52.6 emu/g after ball milling. This decrease was probably resulted from the partial surface oxidation of Mag by ball milling [34,35]. The MS value of 10%TiO_2/Mag decreased to 43.7 emu/g, which could be attributed to the addition of non-magnetic TiO_2 [36]. In spite of the reduction of magnetism, 10%TiO_2/Mag could be rapidly separated from solutions by simply putting an external magnetic field (Fig. 3(b)), which would benefit its recovery and reuse during water treatment.

3.2. Catalytic degradation of cefotaxime

The degradation efficiency and rate of cefotaxime in various systems were tested to determine the catalytic activities of the synthesized samples. All systems were carried out at near neutral pH of 5.6, and this pH was inherent in reaction solutions with no further adjustment. As displayed in Fig. 4 and S3, the adsorption of cefotaxime on all samples almost can be ignored.

In Fenton reaction without UV light, the degradation efficiency and rate of cefotaxime within 60 min catalyzed by ball-milled Mag (14.8% and 0.0024 min^{-1}) were quite similar to those catalyzed by natural Mag (14.0% and 0.0022 min^{-1}) (Fig. 4(a) and S4(a)). In the absence of UV irradiation, H_2O_2 cannot be decomposed by TiO_2, so the degradation of cefotaxime in the TiO_2(P25)+H_2O_2 and TiO_2(ball-milled)+H_2O_2 systems was near to negligible (Fig. S3). In the TiO_2/Mag+H_2O_2 systems, when the loaded content of TiO_2 rose from 3% to 15%, the degradation rate of cefotaxime increased from 0.0055 to 0.0105 min^{-1} (Fig. S4(a)). According to VSM results (Fig. 3(a)), the magnetism of Mag would decrease with the addition of TiO_2, which was beneficial to the dispersion of TiO_2/Mag composites in solutions and correspondingly improved the Fenton degradation of cefotaxime.

During photocatalytic processes (without H_2O_2), when natural or ball-milled Mag was used as the catalyst, the degradation of cefotaxime was fairly poor (Fig. 4(b) and S4(b)). The band gap of Mag was only 0.1 eV, and it generally considered as a poor photocatalyst [37]. Both the TiO_2(P25)-based and TiO_2(ball-milled)-based photocatalytic systems can degrade cefotaxime, and the degradation efficiency and rate within 60 min were 65.6% and 0.0174 min^{-1} for the former as well as 52.6% and 0.0122 min^{-1} for the latter (Fig. S3). The photocatalytic activity of TiO_2 declined mildly after ball milling, which should be attributed to the decrease of its crystallinity (Fig. 1). TiO_2/Mag composites showed much weaker photocatalytic activities

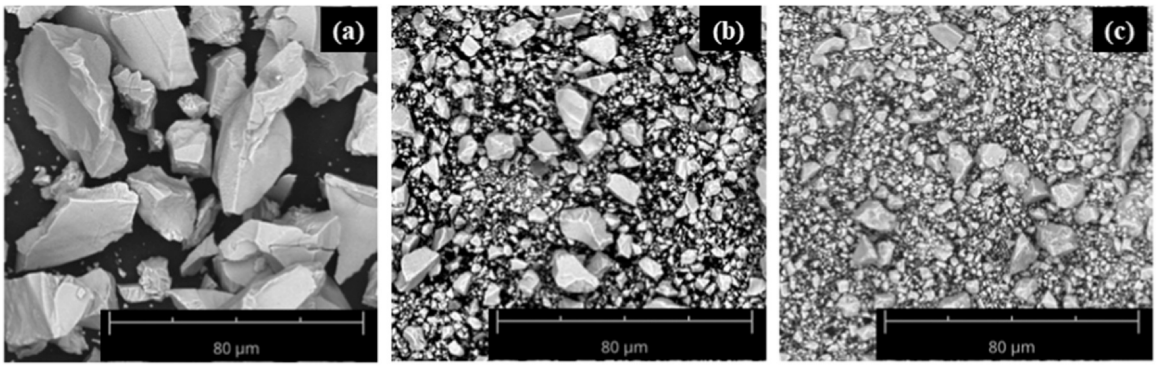

Fig. 2. SEM images of Mag(natural) (a), Mag(ball-milled) (b), and 10%TiO_2/Mag (c).

than TiO_2, while those activities gradually increased with rising TiO_2 content (Fig. 4(b) and S4(b)). Clearly, the photocatalytic activities of TiO_2/Mag composites should increase from the TiO_2 portion.

In photo-Fenton systems, the degradation efficiency of cefotaxime was significantly enhanced as compared with the other two systems (i.e., Fenton reaction and photocatalytic system). After 60 min of photo-Fenton systems, 39.6% and 52.5% of cefotaxime could be removed with the catalyst of natural and ball-milled Mag (Fig. 4(c)). Ball-milled Mag has smaller particle size than natural Mag (Fig. 2(a) and (b)), resulting in better photo-Fenton catalytic activity. TiO_2(P25) presented good catalytic activity in the UV+TiO_2(P25) +H_2O_2 system (Fig. S3), because photo-generated electrons can activate H_2O_2 to produce ·OH (Eq. (2)) and the separation of electron–hole pairs is promoted concurrently [38,39].

$$H_2O_2 + e^- \rightarrow OH^- + \cdot OH \quad (2)$$

Nevertheless, the ball milling process evidently reduced the reactivity of TiO_2, which possibly still due to the decreased crystallinity (Fig. 1). From Fig. 4(c), all TiO_2/Mag composites had good photo-Fenton catalytic activities, and the degradation efficiency of cefotaxime reached 100% within 60 min except 3%TiO_2/Mag (95.3%). With the enhancement of TiO_2 content from 3% to 15%, the degradation rate of cefotaxime in photo-Fenton systems catalyzed by TiO_2/Mag composites increased from 0.0477 to 0.1195 min^{-1} (Fig. 4(d)). These results well revealed the combination of TiO_2 with Mag can obtain a synergistic effect for photo-Fenton system. In particular, the photo-Fenton degradation rate of cefotaxime catalyzed by 10%TiO_2/Mag was 11.6 and 8.2 times higher than that by natural and ball-milled Mag, respectively. Although TiO_2(P25) also showed high degradation rate on cefotaxime (0.0865 min^{-1}) (Fig. S3(b)) when compared to 10%TiO_2/Mag (0.0895 min^{-1}) (Fig. 4(d)), its cost is markedly higher than that of Mag (close to 1000 times), suggesting 10%TiO_2/Mag is more cost-effective photo-Fenton catalyst. Additionally, in degrading environmental hormone bisphenol A, 10%TiO_2/Mag also showed a high photo-Fenton catalytic activity (Fig. S5), which further demonstrated its good applicability in water treatment.

TOC removal efficiency of cefotaxime during catalytic processes was further examined to inspect the catalytic activities of samples. As displayed in Fig. S6, only 5.6% and 5.8% of TOC removal efficiencies were obtained after 60 min of the photo-Fenton systems catalyzed by natural and ball-milled Mag. Comparatively, the UV +10%TiO_2/Mag+H_2O_2 system achieved a higher mineralization at 25.1%, which was also better than those in the UV+10%TiO_2/Mag (2.5%) and 10%TiO_2/Mag+H_2O_2 (4.1%) systems. The results indicated the high photo-Fenton reactivity of 10%TiO_2/Mag.

In summary, the high catalytic activities of TiO_2/Mag composites in photo-Fenton systems should stem from the effective combination of the TiO_2-based photocatalysis and Mag-based Fenton reaction. Given by above evidences, we predict Fe(III) of Mag can capture photo-generated electrons from TiO_2, which subsequently accelerate Fe(II)/Fe(III) cycle in Fenton reaction and inhibit the recombination of electron-hole pairs. The small band gap of Mag is also instrumental in the rapid transfer of photogenerated electrons from TiO_2 to Mag and then to H_2O_2. As a result, both the photocatalysis of TiO_2 and Fenton reaction of Mag were boosted. In a Fe_3O_4@rGO@TiO_2-catalyzed photo-Fenton degradation of methylene blue, Yang et al.

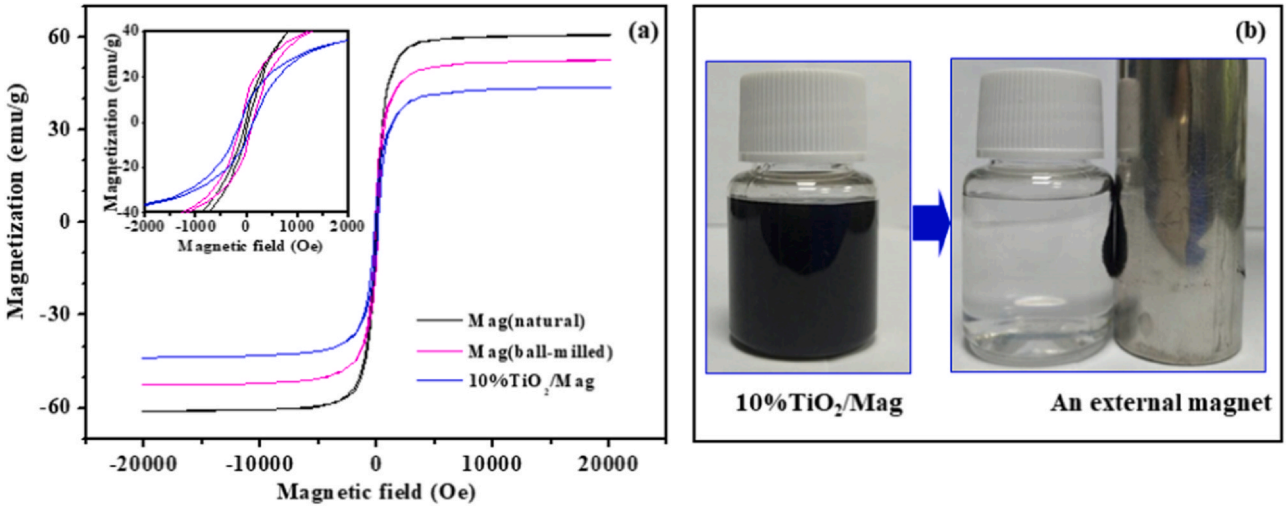

Fig. 3. Room temperature magnetic hysteresis loops of Mag(natural), Mag(ball-milled), and 10%TiO_2/Mag (Inset at the left upper is the corresponding enlarged magnetic hysteresis loop in a low magnetic field.) (a), and magnetic separation for 10%TiO_2/Mag by an external magnet (b).

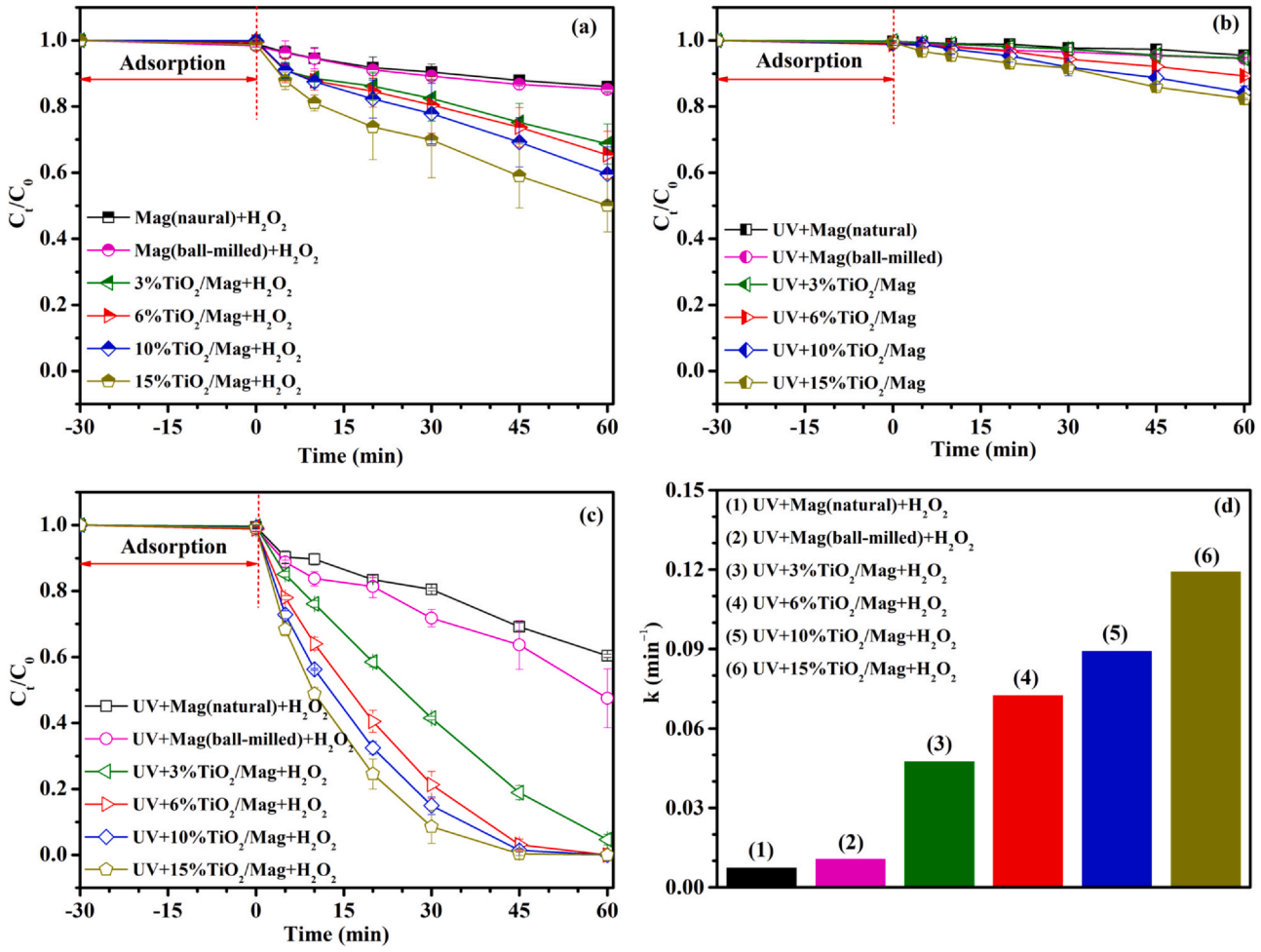

Fig. 4. The degradation efficiency of cefotaxime in the catalyst+H_2O_2 (a), UV+catalyst (b), and UV+catalyst+H_2O_2 (c) systems, as well as the corresponding degradation rate for the UV+catalyst+H_2O_2 system (d).

[11] put forward a similar hypothesis, but gave no sufficient evidence to prove it. In the follow-up, we would confirm the predicted synergistic mechanism in the UV+TiO_2/Mag+H_2O_2 system by investigating the decomposition of H_2O_2, production of ·OH, and generation of Fe(II) in solutions.

The recycling experiments related to the photo-Fenton degradation of cefotaxime were conducted to evaluate the long-term stability of 10%TiO_2/Mag. After four consecutive cycles, the UV +10%TiO_2/Mag+H_2O_2 system could still almost completely remove cefotaxime within 60 min (Fig. 5). Therefore, 10%/TiO_2/Mag should

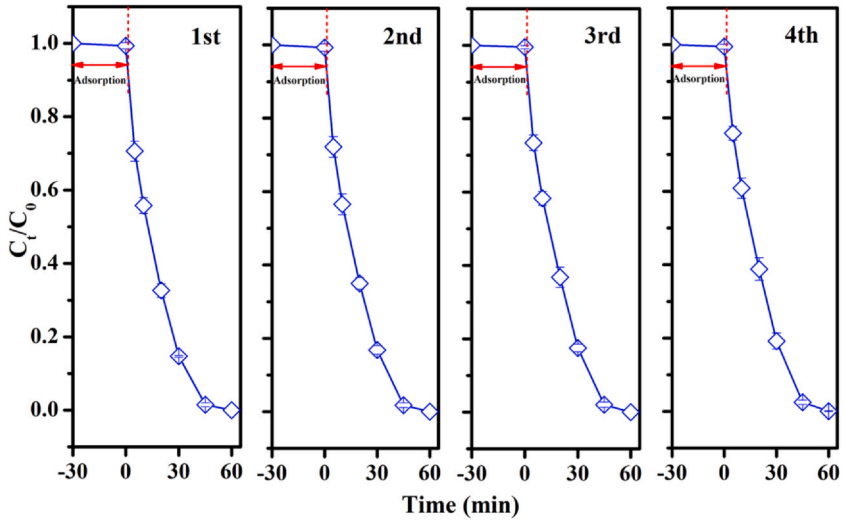

Fig. 5. The cyclic utilization of 10%TiO_2/Mag in the UV+10%TiO_2/Mag+H_2O_2 system for the degradation of cefotaxime.

have good stability, which is of great significance for environmental pollution remediation.

3.3. Effects of initial pH on catalytic systems

In degrading cefotaxime, with the catalyst of natural Mag, ball-milled Mag, and 10%TiO_2/Mag, the effects of initial pH at 5.6, 4.0, and 3.0 on photo-Fenton systems were explored (Fig. 6). When initial pH decreased from 5.6 to 3.0, all the tested photo-Fenton systems appeared rapid enhancements for the degradation of cefotaxime. Specifically, the degradation rate increased from 0.0077 to 0.1969 min^{-1} by natural Mag, from 0.0109 to 0.2094 min^{-1} by ball-milled Mag, and from 0.0895 to 0.2229 min^{-1} by 10%TiO_2/Mag (Fig. 6(d)). The reasons for the higher catalytic activity at the lower pH include the following three aspects: the activation of H_2O_2 by Fe (II) is facilitated by the lower pH, resulting in more ·OH for the degradation of pollutants; the oxidation potential of ·OH also improves, which is nearly 1.9 V at pH of 7.0 and increases to 2.65–2.80 V at pH of 3.0; the more dissolved fraction of iron species, to some extent, accelerates Fenton reaction [24,40,41]. The effects of initial pH on photo-Fenton system catalyzed by natural Mag were similar to those by ball-milled Mag, despite the former photo-Fenton activity was always slightly lower than that of the later (Fig. 6(a) and (b)). Both the Mag(ball-milled)-catalyzed and 10%TiO_2/Mag-catalyzed photo-Fenton systems at pH of 3.0 could basically remove cefotaxime within 30 min, and the degradation efficiency reached 99.8% and 100%, respectively (Fig. 6(b) and (c)). By comparison, when the photo-Fenton systems were at pH of 5.6, which was close to neutral pH, 100% of cefotaxime was degraded by 10%TiO_2/Mag within 60 min, but the degradation efficiency by ball-milled Mag was only 52.5%. Thus, in comparison with ball-milled Mag, 10%TiO_2/Mag has relatively higher photo-Fenton catalytic activity at higher pH even near neutral.

3.4. Effects of H_2O_2 concentration on catalytic systems

The concentration of initial H_2O_2 is an important factor for catalytic systems. In the photo-Fenton systems catalyzed by natural and ball-milled Mag, the degradation of cefotaxime was hardly affected by the concentration of initial H_2O_2 (Fig. 7(a)(b) and S7(a)(b)). A possible explanation was that, natural and ball-milled Mag were of micron scale (at about 10–50 μm and less than 20 μm, respectively), and their small SSA values led to finite contact with H_2O_2, resulting in low utilization of H_2O_2. In contrast, during a photo-Fenton process based on Fe_3O_4 nanoparticles with 40–100 nm particle size, Pastrana-Martínez et al. found the TOC removal efficiency of diphenhydramine enhanced from 25% to 78% as raising H_2O_2 concentration from 1 to 16 mmol/L [42].

In the UV+10%TiO_2/Mag+H_2O_2 system, when the concentration of initial H_2O_2 increased from 1 to 10 mmol/L, the degradation of cefotaxime enhanced correspondingly (Fig. 7(c) and (d)). This was probably because the decomposition of H_2O_2 generated more ·OH to effectively react with contaminants [42,43]. However, further increase in H_2O_2 concentration from 10 to 15 mmol/L gave rise to a

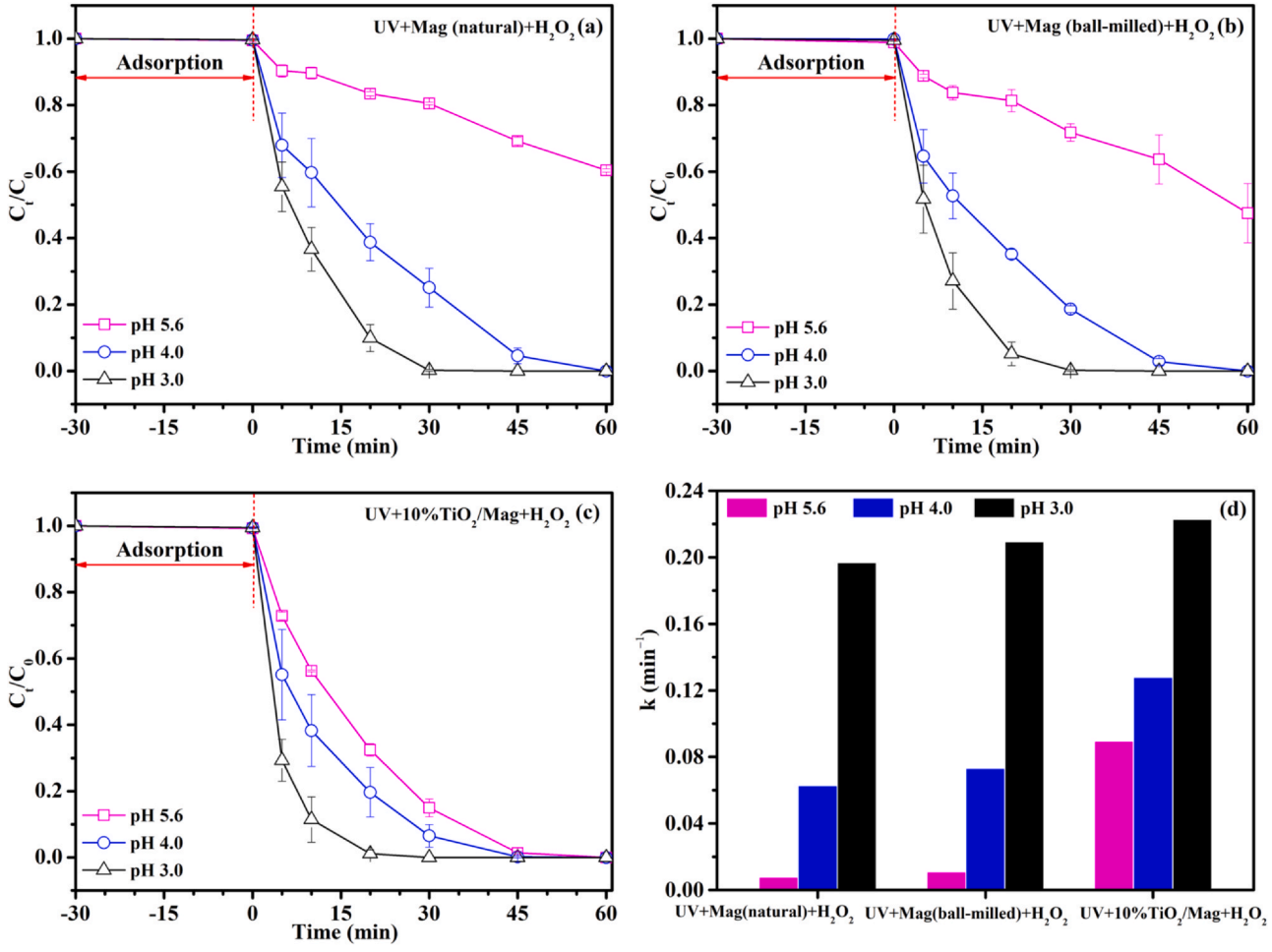

Fig. 6. With various initial pH, the degradation efficiency of cefotaxime in the UV+Mag(natural)+H_2O_2 (a), UV+Mag(ball-milled)+H_2O_2 (b), and UV+10%TiO_2/Mag+H_2O_2 (c) systems, as well as the corresponding degradation rate for these systems (d).

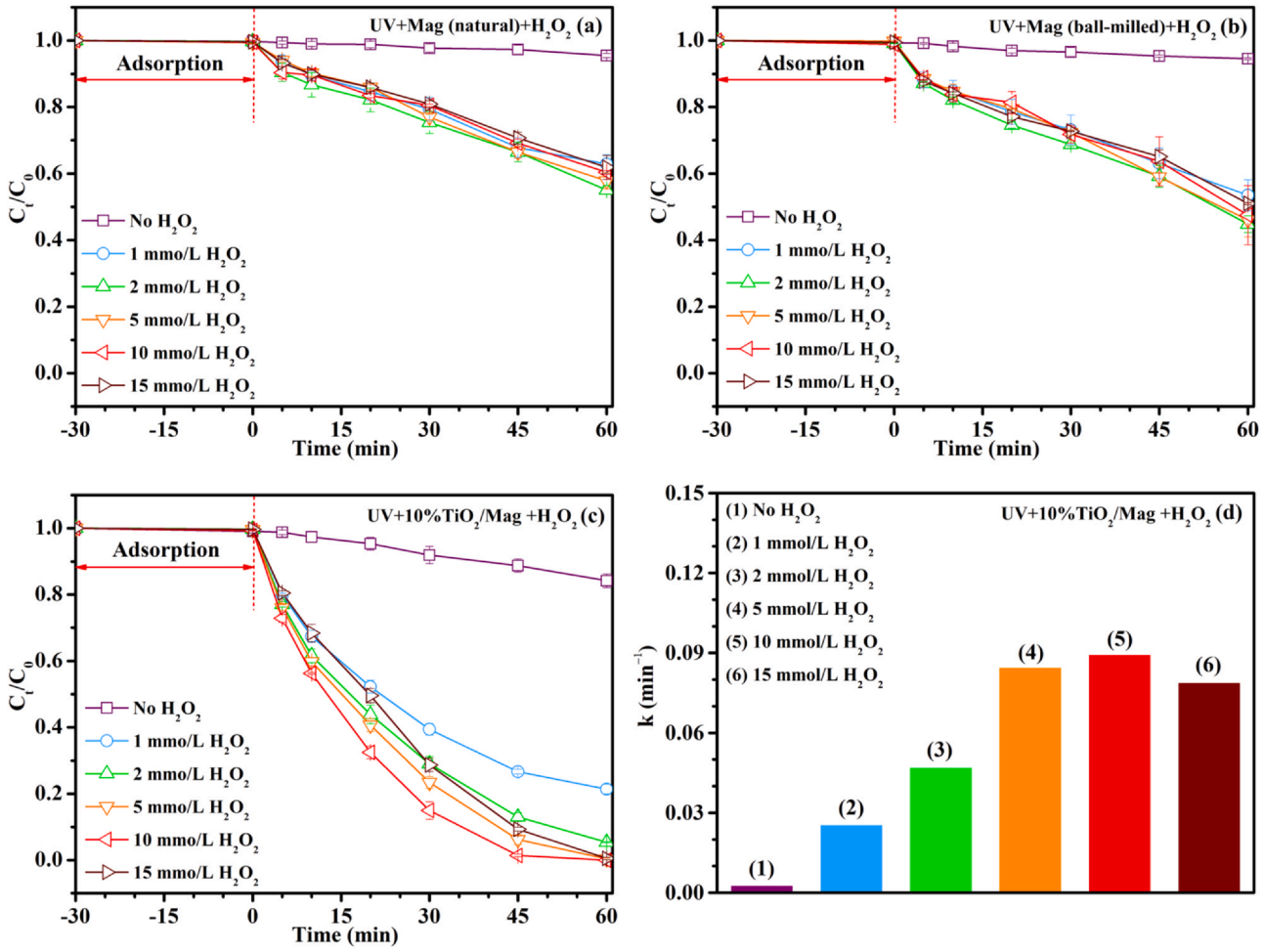

Fig. 7. In the presence of various concentrations H_2O_2, the degradation efficiency of cefotaxime in the UV+Mag(natural)+H_2O_2 (a), UV+Mag(ball-milled)+H_2O_2 (b), and UV +10%TiO_2/Mag+H_2O_2 systems, as well as the corresponding degradation rate for the UV+10%TiO_2/Mag+H_2O_2 system (d).

decreased degradation of cefotaxime. The reasons might be that, excessive H_2O_2 not only quenched h^+ or ·OH (Eqs. (3), (4) and (5)) to produce HO_2·, H_2O, or O_2 with less oxidation potential [44], but also competed with contaminants for reactive sites on the surface of catalysts to form "chromatographic peaking effect" [45,46].

$$H_2O_2 + h^+ \rightarrow HO_2\cdot + H^+ \quad (3)$$

$$H_2O_2 + \cdot OH \rightarrow HO_2\cdot + H_2O \quad (4)$$

$$HO_2\cdot + H_2O_2 \rightarrow O_2 + H_2O \quad (5)$$

As a result, the optimum concentration of initial H_2O_2 was 10 mmol/L.

Even if only 1 mmol/L H_2O_2 was adopted into photo-Fenton system, 78.6% of cefotaxime could be degraded by 10%TiO_2/Mag (Fig. 7(c)), which was much better than that by natural and ball-milled Mag using 10 mmol/L H_2O_2 (39.5% and 52.5%) (Fig. 7(a) and (b)). Besides, the degradation rate of cefotaxime in the UV+10%TiO_2/Mag+H_2O_2 system with 10 mmol/L H_2O_2 showed an obvious enhancement to 0.0895 min^{-1}, when compared to that with no H_2O_2 (0.0028 min^{-1}) (Fig. 7(d)). The enhanced value between these two degradation rates of cefotaxime (0.0867 min^{-1}) was visibly higher than those in the UV+Mag(natural)+H_2O_2 and UV+Mag(ball-milled) +H_2O_2 systems (0.0070 and 0.0101 min^{-1}) (Fig. S7 (a) and (b)). Clearly, 10%TiO_2/Mag has a better efficient utilization of H_2O_2 in comparison with natural and ball-milled Mag. These results supported our prediction that, photo-generated electrons from TiO_2 can accelerate the reduction of Fe(III) to Fe(II), which help to produce more ·OH via the reaction between Fe(II) and H_2O_2 (Eq. (6)) and avoid the consumption of H_2O_2 by Fe(III) (Eq. (7)) [47], thereby leading to efficient utilization of H_2O_2 by 10%TiO_2/Mag.

$$Fe(II) + H_2O_2 \rightarrow Fe(III) + \cdot OH + OH^- \quad (6)$$

$$Fe(III) + H_2O_2 \rightarrow Fe(II) + HO_2\cdot + H^+ \quad (7)$$

3.5. Decomposition of H_2O_2 and production of ·OH

The decomposition of H_2O_2 was measured to further estimate the utilization of H_2O_2 in catalytic systems. After 60 min of UV irradiation, 34.2% of H_2O_2 could be decomposed by 10%TiO_2/Mag, which was much higher than that by natural and ball-milled Mag (4.9% and 6.8%) (Fig. 8(a)). This high decomposition of H_2O_2 by 10%TiO_2/Mag and the efficient degradation of cefotaxime in the UV+10%TiO_2/Mag +H_2O_2 system as mentioned above (Fig. 4(c) and (d)) largely indicated the high conversion of H_2O_2 to ·OH. By comparison, without UV irradiation, the decomposition of H_2O_2 by 10%TiO_2/Mag was almost ignored (Fig. 8(a)), suggesting photo-generated electrons from TiO_2 played an important role for high utilization of H_2O_2 by 10%TiO_2/Mag.

During catalytic processes, several oxygen reactive species might be formed. To determine their contribution in degrading cefotaxime, scavengers including KI, NaN_3, and BQ were used to quench ·OH, O_2^1, and $\cdot O_2^-$, respectively [27]. With the catalyst of natural and ball-milled Mag, when KI, NaN_3, or BQ was added, the photo-Fenton degradation efficiency of cefotaxime within 60 min decreased from

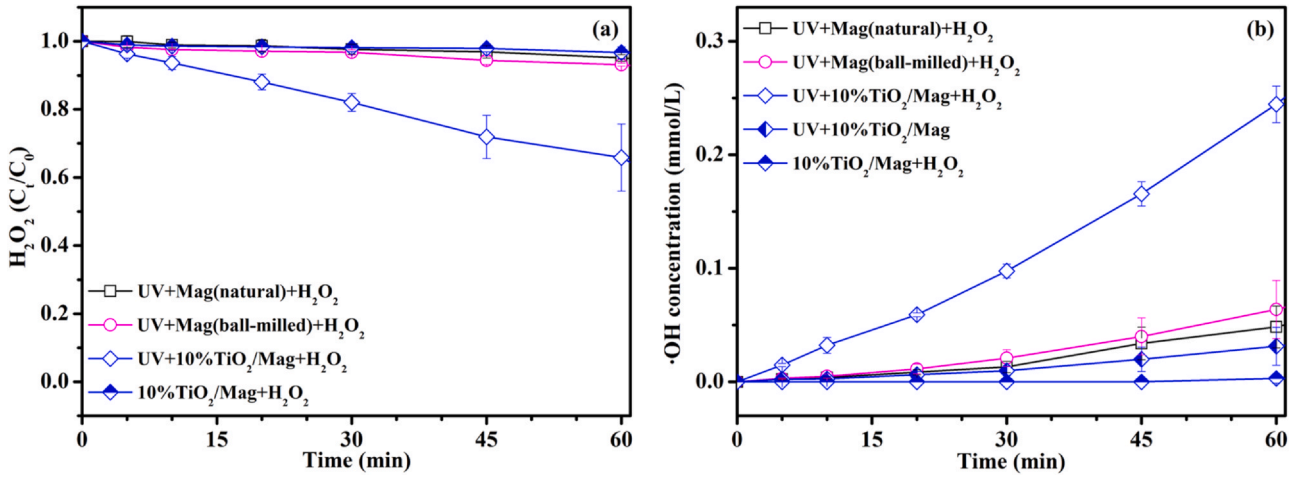

Fig. 8. Monitoring the consumption of H_2O_2 (a) and production of ·OH (b) in various systems.

39.6% to 21.7%, 25.7%, or 33.2%, as well as from 52.5% to 25.5%, 31.8%, or 37.0%, respectively (Fig. S8(a) and (b)). These suggested ·OH was important for the degradation, but the role of O_2^1 and $\cdot O_2^-$ cannot be ignored. Besides, the addition of KI resulted in a more obvious decreased photo-Fenton degradation efficiency of cefotaxime catalyzed by 10%TiO_2/Mag as compared with NaN_3 and BQ (Fig. S8(c)), indicating the dominant contribution of ·OH. Above different results among the three tested catalysts probably suggested that photo-generated electrons from TiO_2 was beneficial to the production of ·OH for 10%TiO_2/Mag.

Given by the important role of ·OH for the degradation of cefotaxime, the production of ·OH in catalytic systems was also quantified. When natural Mag, ball-milled Mag, or 10%TiO_2/Mag was used as the catalyst in photo-Fenton system, 0.049, 0.064, or 0.244 mmol/L ·OH was produced within 60 min, respectively (Fig. 8(b)). The production of ·OH by 10%TiO_2/Mag was the best among them, proving its highly efficient photo-Fenton catalytic activity once again. Moreover, the production of ·OH in the UV+10%TiO_2/Mag and 10%TiO_2/Mag+H_2O_2 systems was as low as to 0.031 and 0.003 mmol/L, respectively (Fig. 8(b)). This result further demonstrated effective combination of the TiO_2-based photocatalysis and Mag-based Fenton reaction in the UV+10%TiO_2/Mag+H_2O_2 system.

3.6. Generation of Fe(II) in solutions

To verify the conversion of Fe(II)/Fe(III), the generation of Fe(II) in solutions during catalytic degradation of cefotaxime was tracked. In adsorption-desorption equilibrium period without UV light and H_2O_2, 0.986–1.099, 0.503–0.628, and 0.258–0.308 mg/L Fe(II) was released from natural Mag, ball-milled Mag, and 10%TiO_2/Mag within 30 min, respectively (Fig. 9). These relative high releases of Fe(II) might be attributed to the strong solubility of Mag in aqueous medium [47]. But it was evident that the ball milling process improved the stability of Mag and the combination of TiO_2 with Mag could further strengthen such stability.

In Fenton reaction without UV light, the generation of Fe(II) from all of the tested catalysts was quite low (Fig. 9), probably because Fe(II) would be oxidized rapidly by H_2O_2 once it was in contact with H_2O_2. In photocatalytic system without H_2O_2, the concentration of Fe(II) in solutions within 120 min showed an enhancement from 1.099 to 1.576 mg/L by natural Mag and 0.628–1.193 mg/L by ball-milled Mag (Fig. 9). In addition to the direct release of Fe(II) from catalysts, the photolysis of Fe(III) under UV illumination could generate Fe(II) as well [48]. The enhanced generation of Fe(II) from 0.258 to 0.948 mg/L within 120 min of the UV+10%TiO_2/Mag system (0.690 mg/L) was higher than that of the UV+Mag(natural)

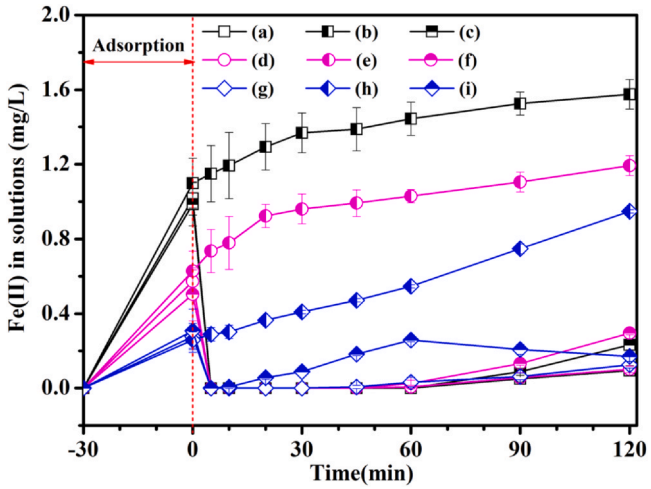

Fig. 9. The generation of Fe(II) in solutions for the UV+Mag(natural)+H_2O_2 (a), UV+Mag(natural) (b), Mag(natural)+H_2O_2 (c), UV+Mag(ball-milled)+H_2O_2 (d), UV+Mag(ball-milled) (e), Mag(ball-milled)+H_2O_2 (f), UV+10%TiO_2/Mag+H_2O_2 (g), UV+10%TiO_2/Mag (h), and 10%TiO_2/Mag+H_2O_2 (i) systems.

(0.477 mg/L) and UV+Mag(ball-milled) systems (0.565 mg/L). The result signified photo-generated electrons from TiO_2 could quicken the reduction of Fe(III) to Fe(II) and then promote the conversion of Fe(II)/Fe(III).

In photo-Fenton systems, the generation of Fe(II) from natural and ball-milled Mag increased gradually as the reaction proceeding (Fig. 9). It might be explained by that, Fe(II) which was produced through the photolysis of Fe(III) and released from catalysts cannot be completely consumed by H_2O_2 in time. The UV+10%TiO_2/Mag+H_2O_2 system in the first 60 min also showed an increasing generation of Fe(II), but such generation after 60 min decreased by degrees. This peaked time at 60 min was consistent with the complete removal time of cefotaxime (Fig. 4(c)). As stated previously [49,50], although the formation of complexes between Fe(II) and organic intermediates in solutions impeded the reaction of Fe(II) with H_2O_2, when contaminants was completely degraded, organic intermediates would continue to mineralize and then enabled Fe(II) which was separated from the complexes to react with H_2O_2.

3.7. Synergistic mechanism in the UV+TiO_2/Mag+H_2O_2 system

On the basis of above experimental results, TiO_2/Mag composites showed high photo-Fenton catalytic activities in degrading

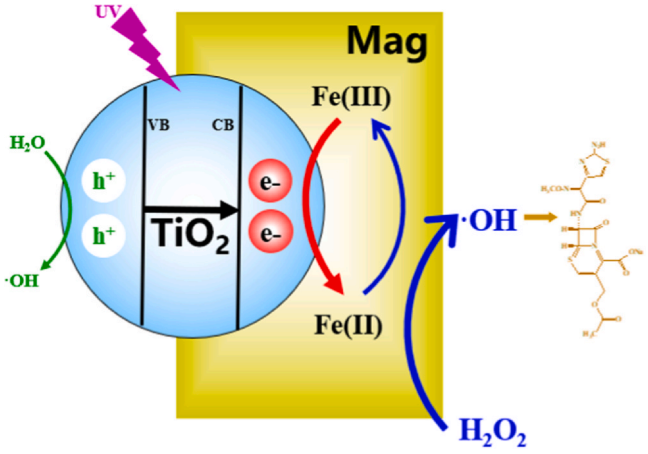

Fig. 10. Schematic diagram in the UV+TiO_2/Mag+H_2O_2 system for the degradation of cefotaxime.

cefotaxime, and the possible synergistic mechanism for the UV +TiO_2/Mag+H_2O_2 system was schematically illustrated in Fig. 10. Under UV irradiation, photo-generated electrons from the TiO_2-based photocatalysis could be trapped by Fe(III) of Mag, advancing the separation of electrons and holes. Since the two following reasons, Fe(III) of Mag should be the major trapper of photo-generated electrons: firstly, the electrode potential of Fe(III) at near neutral pH (E^0 (Fe(III)/Fe(II)) = +0.38 V vs. SHE, SHE refers to standard hydrogen electrode) is very close to that of H_2O_2 (E^0 (H_2O_2/·OH) = +0.39 V vs. SHE) and obviously higher than that of O_2 ((E^0 (O_2/·O_2^-) = −0.18 V vs. SHE)) [51], so photo-generated electrons should prefer to be transferred to Fe(III) of Mag and H_2O_2; secondly, the direct solid-solid contact of Mag and TiO_2 on TiO_2/Mag composites can be conducive to transferring photo-generated electrons to Fe(III) of Mag. The small band gap of Mag at 0.1 eV was also instrumental in the rapid transfer of photo-generated electrons. Concurrently, the trap of photo-generated electrons by Mag contributed to accelerating the redox cycling of Fe(II)/Fe(III) in Fenton reaction, because the reduction of Fe(III) by H_2O_2 (Eq. (7)) is always the major rate-limiting step and its second-order rate is lower than that of the reaction between Fe(II) and H_2O_2 (Eq. (6)) [3,14,52]. Through Fe(II)/Fe(III) cycle, photo-generated electrons would be continuously transferred from TiO_2 to H_2O_2, and then promoted the decomposition of H_2O_2 to produce ·OH for the degradation of cefotaxime. In addition, photo-generated holes could also remove a small amount of cefotaxime by virtue of direct oxidation and the formation of ·OH from the reaction between holes and water. Eventually, cefotaxime was efficiently degraded.

4. Conclusions

In this study, a facile ball milling approach was applied to synthesize TiO_2/Mag composites from precursors of commercial TiO_2 and natural magnetite. The mineral phases of TiO_2 and Mag had no alter after ball milling. In view of good magnetism, TiO_2/Mag composites could be rapidly separated from solutions by simply putting an external magnetic field. During the degradation of cefotaxime, TiO_2/Mag composites showed highly efficient photo-Fenton catalytic activities. The degradation rate by 10%TiO_2/Mag at near neutral pH of 5.6 was about 11.6 and 8.2 times as high as that by natural and ball-milled Mag, and was quite similar to that by commercial TiO_2. Considering TiO_2 was very costly in comparison with Mag, 10%TiO_2/Mag should be more cost-effective catalyst. After four consecutive cycles, 10%TiO_2/Mag remained good stability, and cefotaxime could be almost completely removed within 60 min. Moreover, as compared to natural and ball-milled Mag, 10%TiO_2/Mag had relatively high photo-Fenton catalytic activity even at low H_2O_2 concentration of 1 mmol/L. The better production of ·OH in the UV+10%TiO_2/Mag +H_2O_2 system (0.244 mmol/L) than that in the UV+Mag(natural) +H_2O_2 and UV+Mag(ball-milled)+HU_2O_2 systems (0.049 and 0.064 mmol/L) further indicated the efficient utilization of H_2O_2 by 10%TiO_2/Mag.

The highly efficient photo-Fenton catalytic activity of 10%TiO_2/Mag should be attributed to effective synergy between the TiO_2-based photocatalysis and Mag-based Fenton reaction. In brief, Fe (III) of Mag could capture photo-generated electrons from TiO_2, which accelerated Fe(II)/Fe(III) cycle in Fenton reaction, separation of electron-hole pairs in photocatalysis, decomposition of H_2O_2, and production of ·OH, resulting in effectual removal of cefotaxime. For practical application in water treatment, TiO_2/Mag composites have the following advantages: high photo-Fenton catalytic activity, facile preparation, cost-effective, easy magnetic separation, good stability, suitable for near neutral pH, and efficient utilization of H_2O_2.

CRediT authorship contribution statement

Qi Jiang: Methodology, Formal analysis, Data curation, Writing - original draft. **Runliang Zhu**: Conceptualization, Writing - review & editing, Supervision, Project administration.

Declaration of Competing Interest

The authors declare that they have no known competing financial interests or personal relationships that could have appeared to influence the work reported in this paper.

Acknowledgements

This study was financially supported by the National Natural Science Foundation of China (Grant no. 41872044).

Appendix A. Supporting information

Supplementary data associated with this article can be found in the online version at doi:10.1016/j.jallcom.2021.158670.

References

[1] S.R. Pouran, A.A.A. Raman, W. Daud, Review on the application of modified iron oxides as heterogeneous catalysts in Fenton reactions, J. Clean. Prod. 64 (2014) 24–35.
[2] A. Mirzaei, Z. Chen, F. Haghighat, L. Yerushalmi, Removal of pharmaceuticals from water by homo/heterogonous Fenton-type processes - a review, Chemosphere 174 (2017) 665–688.
[3] A.V. Vorontsov, Advancing Fenton and photo-Fenton water treatment through the catalyst design, J. Hazard. Mater. 372 (2019) 103–112.
[4] M. Munoz, Z.M. de Pedro, J.A. Casas, J.J. Rodriguez, Preparation of magnetite-based catalysts and their application in heterogeneous Fenton oxidation - a review, Appl. Catal. B Environ. 176 (2015) 249–265.
[5] L. Clarizia, D. Russo, I. Di Somma, R. Marotta, R. Andreozzi, Homogeneous photo-Fenton processes at near neutral pH: a review, Appl. Catal. B Environ. 209 (2017) 358–371.
[6] N. Klamerth, S. Malato, A. Aguera, A. Fernandez-Alba, Photo-Fenton and modified photo-Fenton at neutral pH for the treatment of emerging contaminants in wastewater treatment plant effluents: a comparison, Water Res. 47 (2013) 833–840.
[7] A.D. Bokare, W. Choi, Review of iron-free Fenton-like systems for activating H_2O_2 in advanced oxidation processes, J. Hazard. Mater. 275 (2014) 121–135.
[8] S.O. Ganiyu, M.H. Zhou, C.A. Martinez-Huitle, Heterogeneous electro-Fenton and photoelectro-Fenton processes: a critical review of fundamental principles and application for water/wastewater treatment, Appl. Catal. B-Environ. 235 (2018) 103–129.
[9] X.C. Liu, Y.Y. Zhou, J.C. Zhang, L. Luo, Y. Yang, H.L. Huang, H. Peng, L. Tang, Y. Mu, Insight into electro-Fenton and photo-Fenton for the degradation of antibiotics: mechanism study and research gaps, Chem. Eng. J. 347 (2018) 379–397.
[10] J.R. Kim, E. Kan, Heterogeneous photo-Fenton oxidation of methylene blue using CdS-carbon nanotube/TiO_2 under visible light, J. Ind. Eng. Chem. 21 (2015) 644–652.

[11] X.L. Yang, W. Chen, J.F. Huang, Y. Zhou, Y.H. Zhu, C.Z. Li, Rapid degradation of methylene blue in a novel heterogeneous Fe_3O_4@rGO@TiO_2-catalyzed photo-Fenton system, Sci. Rep. 5 (2015) 10632.
[12] M. Yoon, Y. Oh, S. Hong, J.S. Lee, R. Boppella, S.H. Kim, F.M. Mota, S.O. Kim, D.H. Kim, Synergistically enhanced photocatalytic activity of graphitic carbon nitride and WO_3 nanohybrids mediated by photo-Fenton reaction and H_2O_2, Appl. Catal. B Environ. 206 (2017) 263–270.
[13] Y. Cheng, Y. Li, G.B. Ji, B. Quan, X.H. Liang, Z.X. Zhao, J.M. Cao, Y.W. Du, Magnetic and electromagnetic properties of Fe_3O_4/Fe composites prepared by a simple one-step ball-milling, J. Alloy. Compd. 708 (2017) 587–593.
[14] M. Usman, J.M. Byrne, A. Chaudhary, S. Orsetti, K. Hanna, C. Ruby, A. Kappler, S.B. Haderlein, Magnetite and green rust: synthesis, properties, and environmental applications of mixed-valent iron minerals, Chem. Rev. 118 (2018) 3251–3304.
[15] M.C. Pereira, L.C.A. Oliveira, E. Murad, Iron oxide catalysts: Fenton and Fenton-like reactions - a review, Clay Min. 47 (2012) 285–302.
[16] G.S. Parkinson, Iron oxide surfaces, Surf. Sci. Rep. 71 (2016) 272–365.
[17] R. Matta, K. Hanna, S. Chiron, Fenton-like oxidation of 2,4,6-trinitrotoluene using different iron minerals, Sci. Total Environ. 385 (2007) 242–251.
[18] F. Magalhaes, M.C. Pereira, S.E.C. Botrel, J.D. Fabris, W.A. Macedo, R. Mendonca, R.M. Lago, L.C.A. Oliveira, Cr-containing magnetites $Fe_{3-x}Cr_xO_4$: the role of Cr^{3+} and Fe^{2+} on the stability and reactivity towards H_2O_2 reactions, Appl. Catal. A Gen. 332 (2007) 115–123.
[19] X.L. Liang, Y.H. Zhong, S.Y. Zhu, J.X. Zhu, P. Yuan, H.P. He, J. Zhang, The decolorization of acid orange II in non-homogeneous Fenton reaction catalyzed by natural vanadium-titanium magnetite, J. Hazard. Mater. 181 (2010) 112–120.
[20] L. Yu, J.D. Chen, Z. Liang, W.C. Xu, L.M. Chen, D.Q. Ye, Degradation of phenol using Fe_3O_4-GO nanocomposite as a heterogeneous photo-Fenton catalyst, Sep. Purif. Technol. 171 (2016) 80–87.
[21] Y.X. Deng, M.Y. Xing, J.L. Zhang, An advanced TiO_2/Fe_2TiO_5/Fe_2O_3 triple-heterojunction with enhanced and stable visible-light-driven Fenton reaction for the removal of organic pollutants, Appl. Catal. B Environ. 211 (2017) 157–166.
[22] T.Y. Xu, R.L. Zhu, G.Q. Zhu, J.X. Zhu, X.L. Liang, Y.P. Zhu, H.P. He, Mechanisms for the enhanced photo-Fenton activity of ferrihydrite modified with $BiVO_4$ at neutral pH, Appl. Catal. B Environ. 212 (2017) 50–58.
[23] Y. Zhu, R. Zhu, L. Yan, H. Fu, Y. Xi, H. Zhou, G. Zhu, J. Zhu, H. He, Visible-light Ag/AgBr/ferrihydrite catalyst with enhanced heterogeneous photo-Fenton reactivity via electron transfer from Ag/AgBr to ferrihydrite, Appl. Catal. B Environ. 239 (2018) 280–289.
[24] Y.P. Zhu, R.L. Zhu, Y.F. Xi, T.Y. Xu, L.X. Yan, J.X. Zhu, G.Q. Zhu, H.P. He, Heterogeneous photo-Fenton degradation of bisphenol A over Ag/AgCl/ferrihydrite catalysts under visible light, Chem. Eng. J. 346 (2018) 567–577.
[25] T.K. Ghorai, M. Chakraborty, P. Pramanik, Photocatalytic performance of nano-photocatalyst from TiO_2 and Fe_2O_3 by mechanochemical synthesis, J. Alloy. Compd. 509 (2011) 8158–8164.
[26] Q. Jiang, R.L. Zhu, Y.P. Zhu, Q.Z. Chen, Efficient degradation of cefotaxime by a UV +ferrihydrite/TiO_2+H_2O_2 process: the important role of ferrihydrite in transferring photo-generated electrons from TiO_2 to H_2O_2, J. Chem. Technol. Biotechnol. 94 (2019) 2512–2521.
[27] W. Li, S. Zhao, B. Qi, Y. Du, X.H. Wang, M.X. Huo, Fast catalytic degradation of organic dye with air and MoO_3:Ce nanofibers under room condition, Appl. Catal. B-Environ. 92 (2009) 333–340.
[28] P. Zhang, S.H. Yuan, P. Liao, Mechanisms of hydroxyl radical production from abiotic oxidation of pyrite under acidic conditions, Geochim. Cosmochim. Acta 172 (2016) 444–457.
[29] O. Acisli, A. Khataee, S. Karaca, A. Karimi, E. Dogan, Combination of ultrasonic and Fenton processes in the presence of magnetite nanostructures prepared by high energy planetary ball mill, Ultrason. Sonochem. 34 (2017) 754–762.
[30] O. Acisli, A. Khataee, R.D.C. Soltani, S. Karaca, Ultrasound-assisted Fenton process using siderite nanoparticles prepared via planetary ball milling for removal of reactive yellow 81 in aqueous phase, Ultrason. Sonochem. 35 (2017) 210–218.
[31] K. Saitow, T. Wakamiya, 130-fold enhancement of TiO_2 photocatalytic activities by ball milling, Appl. Phys. Lett. 103 (2013) 031916.
[32] P. Zhang, Z.L. Mo, Y.W. Wang, L.J. Han, C. Zhang, G.P. Zhao, Z. Li, One-step hydrothermal synthesis of magnetic responsive TiO_2 nanotubes/Fe_3O_4/graphene composites with desirable photocatalytic properties and reusability, RSC Adv. 6 (2016) 39348–39355.
[33] H.Y. Fu, Y.X. Yang, R.L. Zhu, J. Liu, M. Usman, Q.Z. Chen, H.P. He, Superior adsorption of phosphate by ferrihydrite-coated and lanthanum decorated magnetite, J. Colloid Interface Sci. 530 (2018) 704–713.
[34] S. Fathinia, M. Fathinia, A.A. Rahmani, A. Khataee, Preparation of natural pyrite nanoparticles by high energy planetary ball milling as a nanocatalyst for heterogeneous Fenton process, Appl. Surf. Sci. 327 (2015) 190–200.
[35] A. Hassani, C. Karaca, S. Karaca, A. Khataee, O. Acisi, B. Yilmaz, Enhanced removal of basic violet 10 by heterogeneous sono-Fenton process using magnetite nanoparticles, Ultrason. Sonochem. 42 (2018) 390–402.
[36] M. Kermani, B. Kakavandi, M. Farzadkia, A. Esrafili, S.F. Jokandan, A. Shahsavani, Catalytic ozonation of high concentrations of catechol over TiO_2@Fe_3O_4 magnetic core-shell nanocatalyst: optimization, toxicity and degradation pathway studies, J. Clean. Prod. 192 (2018) 597–607.
[37] Y. Xu, M.A.A. Schoonen, The absolute energy positions of conduction and valence bands of selected semiconducting minerals, Am. Miner. 85 (2000) 543–556.
[38] A.C. Affam, M. Chaudhuri, Degradation of pesticides chlorpyrifos, cypermethrin and chlorothalonil in aqueous solution by TiO_2 photocatalysis, J. Environ. Manag. 130 (2013) 160–165.
[39] Q. Zhang, C.L. Li, T. Li, Rapid photocatalytic decolorization of methylene blue using high photon flux UV/TiO_2/H_2O_2 process, Chem. Eng. J. 217 (2013) 407–413.
[40] L.J. Xu, J.L. Wang, Fenton-like degradation of 2,4-dichlorophenol using Fe_3O_4 magnetic nanoparticles, Appl. Catal. B Environ. 123 (2012) 117–126.
[41] L.W. Hou, L.G. Wang, S. Royer, H. Zhang, Ultrasound-assisted heterogeneous Fenton-like degradation of tetracycline over a magnetite catalyst, J. Hazard. Mater. 302 (2016) 458–467.
[42] L.M. Pastrana-Martinez, N. Pereira, R. Lima, J.L. Faria, H.T. Gomes, A.M.T. Silva, Degradation of diphenhydramine by photo-Fenton using magnetically recoverable iron oxide nanoparticles as catalyst, Chem. Eng. J. 261 (2015) 45–52.
[43] J. Herney-Ramirez, A.M.T. Silva, M.A. Vicente, C.A. Costa, L.M. Madeira, Degradation of acid orange 7 using a saponite-based catalyst in wet hydrogen peroxide oxidation: kinetic study with the Fermi's equation, Appl. Catal. B Environ. 101 (2011) 197–205.
[44] H.L. Otalvaro-Marin, F. Gonzalez-Caicedo, A. Arce-Sarria, M.A. Mueses, J.C. Crittenden, F. Machuca-Martinez, Scaling-up a heterogeneous H_2O_2/TiO_2/solar-radiation system using the Damkohler number, Chem. Eng. J. 364 (2019) 244–256.
[45] D.D. Dionysiou, M.T. Suidan, I. Baudin, J.M. Laine, Effect of hydrogen peroxide on the destruction of organic contaminants-synergism and inhibition in a continuous-mode photocatalytic reactor, Appl. Catal. B Environ. 50 (2004) 259–269.
[46] A. Chatzitakis, C. Berberidou, I. Paspaltsis, G. Kyriakou, T. Sklaviadis, I. Poulios, Photocatalytic degradation and drug activity reduction of chloramphenicol, Water Res. 42 (2008) 386–394.
[47] A. Hassani, M. Karaca, S. Karaca, A. Khataee, O. Acisli, B. Yilmaz, Preparation of magnetite nanoparticles by high-energy planetary ball mill and its application for ciprofloxacin degradation through heterogeneous Fenton process, J. Environ. Manag. 211 (2018) 53–62.
[48] F. Wu, N.S. Deng, Photochemistry of hydrolytic iron (III) species and photo-induced degradation of organic compounds. A minireview, Chemosphere 41 (2000) 1137–1147.
[49] X.P. Wei, H.H. Wu, G.P. He, Y.F. Guan, Efficient degradation of phenol using iron-montmorillonite as a Fenton catalyst: importance of visible light irradiation and intermediates, J. Hazard. Mater. 321 (2017) 408–416.
[50] C.Y. Yuan, Y.P. Chin, L.K. Weavers, Photochemical acetochlor degradation induced by hydroxyl radical in Fe-amended wetland waters: impact of pH and dissolved organic matter, Water Res. 132 (2018) 52–60.
[51] W.H. Koppenol, R.H. Hider, Iron and redox cycling. Do's and don'ts, Free Radic. Biol. Med. 133 (2019) 3–10.
[52] Y.P. Zhu, R.L. Zhu, Y.F. Xi, J.X. Zhu, G.Q. Zhu, H.P. He, Strategies for enhancing the heterogeneous Fenton catalytic reactivity: a review, Appl. Catal. B Environ. 255 (2019) 117739.